# Solar heat in the Brazilian dairy industry: a preliminary economic assessment

**Leonardo F. L. Lemos, Lucas Werner, Thiago T. C. de Souza, Allan R. Starke and Sergio Colle**

LEPTEN, Department of Mechanical Engineering, Federal University of Santa Catarina, Florianópolis (Brazil)

**Abstract**

This study assesses the feasibility of using Solar Heating for Industrial Processes (SHIP) in the Brazilian dairy industry, for both preheating and steam generation. Simulations were carried out in TRNSYS for three SHIP integration concepts to a representative dairy plant at several Brazilian locations. The Levelized Cost of Heat (LCOH) for each concept was calculated and compared to the levelized cost of the system operating only with natural gas. Furthermore, a sensitivity analysis was performed to assess the influence of the discount rate and fuel prices in the profitability of SHIP systems, allowing to calculate how much the costs of SHIP systems must be reduced for solar process heat to be profitable. The results of this analysis may be useful for the development of policies to further the use of renewable energy in the Brazilian dairy industry.

*Keywords: SHIP, dairy industry, TRNSYS, LCOH*

## 1. Introduction

Solar Heating for Industrial Processes (SHIP) has been widely used in applications in the food industry worldwide, since the processes involved require thermal power at low and medium temperatures. In fact, recent studies present the Brazilian food and beverages industry as one of the most promising industries for SHIP in the country (Solar Payback,2018), due to its high heat demand and significant impact in the national GDP.

Despite the potential for its usage, SHIP systems have not yet spread into the Brazilian industry. Some of the main reasons preventing the usage of SHIP solutions are the high cost of solar equipment and unfavorable financing conditions, which make it difficult for such systems to be profitable. Investment costs for SHIP systems still need to decrease so that solar process heat can be a viable alternative to the Brazilian industry.

The Brazilian dairy industry has been selected as a case study to assess the required conditions for SHIP to be economically viable. The dairy industry has the second largest revenue in the Brazilian food and beverages sector (ABIA, 2018) and its heat demand is relatively more stable along the year when compared to other food industries (Goswami et al. 2000).

The magnitude of the cost reduction required for SHIP to be viable depends on the SHIP system performance. That means that SHIP profitability is heavily dependent on the site selected to install solar process heat, the type of collector used and the way that solar collectors are integrated to the industrial process. Other critical factors in SHIP profitability are the discount rate considered and the cost of the conventional fuel that is going to be substituted by solar heat. Assessing the influence of all these listed factors can help policy makers and investors to understand the conditions needed for further usage of solar thermal energy in the Brazilian dairy industry.

## 2. Methodology

### 2.1. Heat demand

To evaluate the use of SHIP in the dairy industry, it is first necessary to estimate an industrial process heat demand that is representative of the dairy sector. For that purpose, the pre-heating and evaporation of condensate was considered. This process consists of a boiler operating at 900 kPa which supplies saturated process steam to a dairy plant. The process condensate returns at a temperature of 45ºC. These pressure and temperature values were chosen based on information presented by Bylund (1995) and in surveys and case studies found in the literature (Appsol, 2014; Mane, 2013; Quijera et al., 2011; Silva, 2014).

Based on the heat energy demand for each dairy product (Appsol, 2014), and on the total yearly amounts of several dairy products produced by the Brazilian industry (FAS-USDA, 2018), a weighted average was calculated to estimate the thermal power required by an average Brazilian dairy plant. By knowing the required thermal power and the


doi:10.18086/swc.2019.12.08 Available at http://proceedings.ises.org

boiler operating conditions, a steam flow was calculated.

2.2. Selected locations

The next step was to simulate SHIP systems to supply the thermal energy required by the average dairy plant from section 2.1. To assess the impact of the location of SHIP systems on its performance and cost, five Brazilian locations were selected. The cities of Juiz de Fora, Goiânia, São Miguel do Oeste and Porto Velho were selected since they are in parts of the country with a high concentration of dairy processing industries. The city of Bom Jesus da Lapa was also selected, due to its high solar irradiation along the year. Typical Meteorological Years (TMYs) were generated for these locations using global irradiance measurements from the National Institute of Meteorology (INMET,2019) together with a separation model previously developed to estimate hourly diffuse and beam irradiance from global irradiance measurements in Brazil (Lemos et al., 2017; Machado et al., 2019).

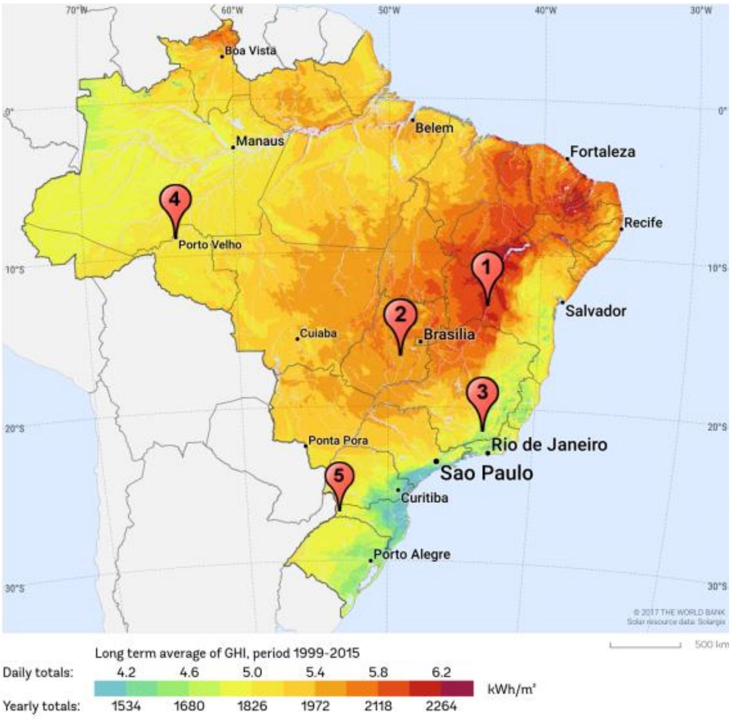


**Fig. 1: Yearly average global horizontal irradiation map in Brazil, with the locations selected for this study marked as follows: 1. Bom Jesus da Lapa, 2. Goiânia, 3. Juiz de Fora, 4. Porto Velho and 5. São Miguel do Oeste. Source: adapted from World Bank Group (2019).**

2.3. Simulated systems description

Three different solar process heat systems were simulated: two for pre-heating of condensate and one for steam generation. The pre-heating systems are schematically shown in Figs. 2a and 2b, where condensate water is heated by the solar field and then directed to the boiler for evaporation. In the third system, illustrated in Fig. 2c, the solar field operates in parallel with the industrial boiler to generate steam. The efficiency of the boiler was assumed to be 78%.

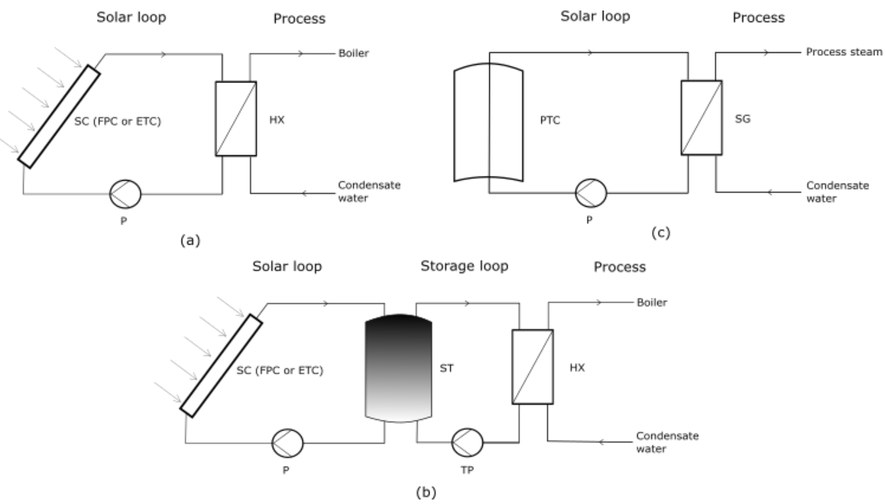


**Fig. 2: Systems with FPC or ETC without storage (a), with storage (b) and (c) for process steam generation with PTC.**

The first system is composed of either a flat-plate (FPC) or evacuated-tube (ETC) solar collector operating with compressed water, a pump (P) and a heat exchanger (HX). The heat exchanger operates with balanced mass flows, in other words, the water mass flow rate in the solar field is equal to the condensate mass flow rate from the demand. The design logarithmic mean temperature difference at the HX was set to 5 K. To size the system components, the maximum solar irradiance at the analyzed location TMY was used. Thus, by specifying the collector area, the operating temperatures and heat exchanger UA can be calculated, since the design solar irradiance and the cold and hot design mass flow rates are known. More solar collector area results in higher temperatures of the preheated condensate at the HX outlet, since the mass flow in the solar field is matched with the condensate flow in the HX.

The solar collectors selected were the Enertech Enersol HP 70-24 evacuated tube collector and the Arcon HTHEATboost 35/10 flat plate collector (Solar Keymark, 2019). The evacuated tube collectors were simulated in TRNSYS using Type 71, and the flat plate collector was simulated using Type 539 from the TESS library (TESS,2014). The heat exchanger and single-speed pumps were simulated using Types 5b and 3b, respectively. An instance of Type 92 (auxiliary cooling unit) was added at the collector field outlet, in order to simulate a heat removal system in case the field outlet temperature happens to be larger than the maximum allowed collector temperature during simulation. This Type acts as a mathematical equivalent of an overheating prevention system in the solar field. A Type 2b differential controller activates the single-speed field pump based on the temperature difference between the solar field outlet and the demand condensate return temperature.

The second system is similar to the first one, with the addition of a storage tank (ST) and a tank recirculation pump (TP). The storage volume is proportional to the solar field area by a ratio of 0.05 $m^3/m^2$. The mass flow rate in each row of the collector field is equal to the test flow rate of one collector, while the mass flow rates in both sides of the HX are matched. The design collector outlet temperature is calculated by assuming the peak solar irradiance value from the location TMY. The heat exchanger is sized by assuming that the hot water from the storage enters the HX at the calculated design collector outlet temperature, and that the log mean temperature difference in the HX is 5 K. The TRNSYS simulation was executed using the same Types as in the simulation of the system from Fig. 2a, with the addition of Type 534 to simulate the thermal storage tank. The pump that drives the flow between the tank and the heat exchanger is activated by a differential controller that compares the temperature difference between the tank hot outlet and the demand condensate return temperature.

The third system is equipped with a parabolic trough collector (PTC) with Therminol VP-1 as heat transfer fluid and a steam generator (SG) operating in parallel with the conventional boiler that supplies the steam demand. The PTC collector selected was the NEP PolyTrough 1800 (SPF, 2019), which was simulated in TRNSYS by Type 536. As in the previous simulated systems, an instance of Type 92 was used as a mathematical equivalent of an overheating prevention system, in the PTC case the defocusing of collectors. The steam generator was simulated by Type 637a from the TESS library.

## 2.4. LCOH calculations

The Levelized Cost of Heat (LCOH, in €/MWh) of the heat substituted by solar thermal energy was chosen as a figure of merit to compare the different solar designs and technologies at different locations. Its evaluation was based on IEA-SHC Task 54 (Louvet et al, 2017). A parametric analysis was performed with the simulations described in section 2.3, to obtain the effect of collector field area on the LCOH, and to find the optimal field size that delivers the lowest heat cost. The initial investment cost of the system is the sum of the solar field, heat exchanger and storage costs.

The specific initial investment costs for the solar field include the cost of the solar panels, pipes and pumps. The assumed specific cost of the FPC was 315 €/m² (Solar Payback, 2018). For ETC, a price of 475 €/m² was considered, based on a difference in price between ETC and FPC technology (Sokhansefat et al, 2017). An area-dependent equation presented by Tian (2017) was used to calculate the specific cost of the PTC. Plate heat exchanger area-dependent cost equations were obtained from Rahimi and Chua (2017), whereas cost equations for steam generation components were taken from Cortés et al. (2017), Ulrich and Vasudevan (2004). All heat exchanger costs were adjusted by the Chemical Engineering Plant Cost Index (CEPCI). The cost of storage tanks was estimated from IEA-SHC Task 52 (Mauthner and Herkel, 2016). The cost equations used in this work are summarized in Table 1, along with the CEPCI indexes considered.

**Tab. 1: Cost equations and CEPCI for SHIP equipment**

| | **Cost equation (€)** |
|---|---|
| Flat plate collector | $C = 315A$ |
| Evacuated tube collector | $C = 475A$ |
| Parabolic trough collector | $C = \left(1865A^{-0.17}\right)A$ |
| Plate HX | $C = \begin{cases} \left(\frac{€}{USD}\right) * 2 * 1281 * \left(A^{0.4887}\right)\left(\frac{CEPCI_{2017}}{CEPCI_{2002}}\right), & if\ A \leq 18.6\ m^2 \\ \left(\frac{€}{USD}\right) * 2 * 702 * \left(A^{0.6907}\right)\left(\frac{CEPCI_{2017}}{CEPCI_{2002}}\right), & otherwise \end{cases}$ |
| Preheater / Superheater | $PEC_{2004} = \exp\{-0.0062\log(A)^4 + 0.0472\log(A)^3 - 0.0328\log(A)^2 + 0.3631\log(A) + 3.2021\}$ <br> $F_p = 0.0444log(P)^2 + 0.1078log(P) + 0.8534$ <br> $F_{BM}^{\alpha} = 1.3125(F_pF_M) + 1.6875$ <br> $F_M = 3$ <br> $C = \left(\frac{€}{USD}\right) F_{BM}^{\alpha} PEC_{2004} \frac{CEPCI_{2017}}{CEPCI_{2004}}$ |
| Evaporator | $PEC_{2004} = \exp\{0.8674\log(A) + 2.8154\}$ <br> $F_p = 0.1433\log(P)^3 - 0.6387\log(P)^2 + 1.2141\log(P) + 0.2795$ <br> $F_{BM}^{\alpha} = 6.2$ <br> $C = \left(\frac{€}{USD}\right) F_{BM}^{\alpha}\ F_p\ PEC_{2004} \frac{CEPCI_{2017}}{CEPCI_{2004}}$ |
| Storage tank | $C = (403.5(V^{-0.4676}) + 750)\ V$ |
| CEPCI | $CEPCI_{2017} = 567.5$ <br> $CEPCI_{2004} = 444.2$ <br> $CEPCI_{2002} = 395.6$ |

In Table 1, $A$ is the area of the solar field or the HX area, in m², $P$ is the HX operating pressure in barg and $V$ is the tank volume in m³. The ratio €/USD is the conversion factor from US dollars to euros, herein considered equal do 0.88. In order to determine heat exchanger areas, heat transfer coefficients were taken from the VDI Heat Atlas (VDI-Gesellschaft, 2010), and were equal to 775 W/m²K for the plate HX, 675 W/m²K for the preheater and 1150 W/m²K for the evaporator.

Subsidies and incentives to use the solar technology were considered equal to zero. Operation and maintenance costs per year were held constant at 1% of the initial investment. The asset depreciation was considered equal to 10% of initial investment in the first ten years and afterwards equal to zero. The corporate tax rate used was 34%. The residual value was considered zero, and the weighted average cost of capital (WACC) was used as discount rate, as suggested in the guideline by Louvet et al. (2017). An average WACC disregarding inflation equal to 9.43% to renewable energy projects in Brazil was used based on Rocha et al. (2012) in a study of the Brazilian Institute for Applied Economic Research. The period of analysis was 20 years and the generated energy in each year of operation was considered constant throughout the years.

The LCOH of the simulated systems was compared with the levelized cost if all the process heat was supplied by the boiler using natural gas. The purchase and maintenance costs of the boiler were not considered, as it is assumed that the SHIP system is installed to substitute natural gas in a previously installed system. The price assumed for natural gas was 39 €/MWh (Solar Payback, 2018). It is worth mentioning that the LCOH of a heating system using only natural gas is slightly higher than the market price of gas, due to boiler inefficiency. So, the LCOH of natural gas assuming a 78% boiler efficiency is 50 €/MWh. The economic parameters assumed in this work are summarized in Table 2.

**Tab. 2: Economic assumptions**

| Parameter | |
|---|---|
| Subsidies | 0 |
| Operation and maintenance | 1% of initial investment cost (in €) |
| Depreciation | 10% in the first ten years |
| Corporate tax | 34 % |
| Residual value | 0 |
| Discount rate | 9.43% |
| Period of analysis | 20 years |
| Reference cost of fuel | 39 €/MWh |

## 3. Results

In Fig. 3 the LCOH of different systems are shown as a function of collector area and compared with the levelized cost of natural gas. Almost none of the systems whose simulation results are shown in Fig. 3 have presented a lower LCOH than that of natural gas, demonstrating that high SHIP costs relatively to conventional fuels present a challenge to SHIP applications in Brazil. The only exception was the system from Fig. 2a in Bom Jesus da Lapa, which has the highest yearly irradiation among the selected locations, thus resulting in the smaller LCOH among the selected locations.

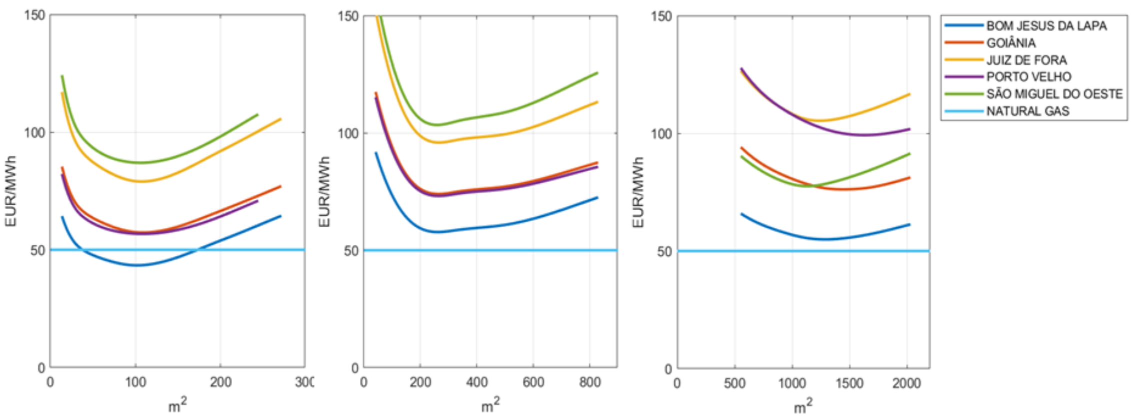


**Fig. 3: LCOH for different simulated systems as a function of collector area. From left to right: system from Fig. 2a using FPC collectors, system from Fig. 2b using ETC collectors, system from Fig. 2c with PTC collectors**

São Miguel do Oeste was the worst location for FPC and ETC systems, while Porto Velho has one of the highest LCOH for the PTC system. Even tough Porto Velho has a slightly higher yearly global irradiation than São Miguel do Oeste, the latter has clearer days while cloudy days are more common in the former. Thus, concentrating systems perform better in São Miguel do Oeste than in Porto Velho.

For a comparison of the profitability of each simulated SHIP system, the influence of discount rate and conventional fuel costs on the payback time of each system is shown in Figs. 4, 5 and 6, for São Miguel do Oeste, Porto Velho and Bom Jesus da Lapa, respectively. In each of these figures, constant payback time curves are plotted for each pair of system integration and collector types. The field areas used to generate these curves were the optimal field areas obtained from Fig. 3. The curves show not only how the site selection for the SHIP system influences the cost of delivered heat, but also show which type of system integration is more profitable at each location.

The curves in Figs. 4, 5 and 6 show how much the solar field cost must be reduced for the system to pay itself, at a given discount rate or a given fuel cost. For instance, in Fig. 4 the blue curve more to the right shows the combination of discount rate and initial investment costs required to obtain a payback time of 5 years for the system shown in Fig.2c operating with PTC collectors. So, in São Miguel do Oeste, if the discount rate is equal to 3 % instead of 9.43%, the initial investment costs must be reduced to 32% of its current value, so that the PTC system can have a payback time of 5 years. For this curve the cost of fuel is maintained constant at 39 €/MWh. Similarly, the orange curves show the influence of fuel and initial investment costs for a constant payback time and fixed discount rate. So, at a discount rate of 9.43%, if conventional fuel prices were up to 74 €/MWh, the initial investment cost of the PTC system would still have to be 51% of its current value in order to achieve a payback time of 5 years. With the fuel price equal to the current price of natural gas and with a discount rate equal to the calculated WACC, a payback of 5 years can be achieved for the PTC system if the cost of initial investment is reduced to around 26% of its current value. For a payback of 2 years, the initial cost must be as low as 11% of its current value. Even greater cost reductions are required for the FPC and ETC systems to achieve payback times of 2 years in São Miguel do Oeste, as evidenced by the other orange curves more to the left.

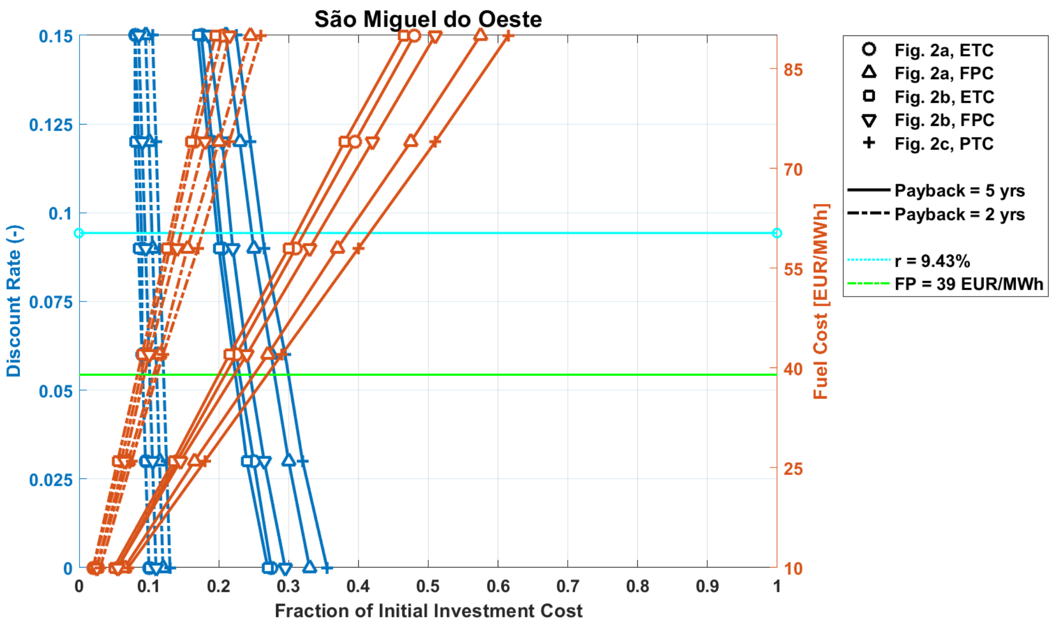


**Fig. 4: Constant payback time curves for each simulated system in São Miguel do Oeste, as a function of the reduction in initial investment cost. Curves in blue show the relationship between the discount rate and initial investment for fixed payback times. Orange curves show the relation between conventional fuel cost and initial investment for fixed payback times.**

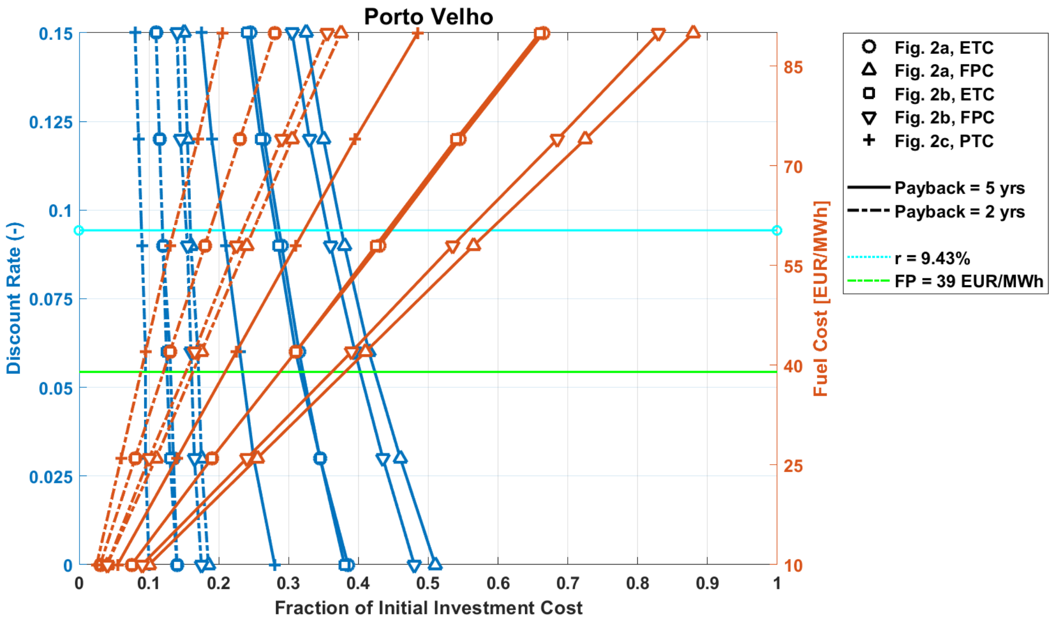


**Fig. 5: Constant payback time curves for each simulated system in Porto Velho, as a function of the reduction in initial investment cost. Curves in blue show the relationship between the discount rate and initial investment for fixed payback times. Orange curves show the relation between conventional fuel cost and initial investment for fixed payback times.**

Thus, in São Miguel do Oeste, the PTC system requires smaller investment cost reductions at fixed discount rate and fuel costs, when compared to fixed collector systems. For Porto Velho (Fig. 5) the opposite is true, with larger investment cost reductions being necessary for PTC to reach payback than for FPC and ETC systems. Even so, significant cost reductions are necessary, usually higher than 50% in most of the scenarios summarized in Fig. 5.

Even in the location with the highest yearly total irradiation, Bom Jesus da Lapa (Fig. 6), the required reduction in investment costs is considerable. For instance, if the initial investment costs were around 41% of its current value, a 5 year payback time for the PTC system shown in Fig. 2c could be achieved if the discount rate was around 6% or if the fuel price is around 42 €/MWh. At the current price of natural gas and the calculated WACC as discount rate, a payback of 5 years can be achieved if the cost of the initial investment is reduced to around 37% of its current value. For a payback of 2 years, the field cost must be as low as 16% of its current value.

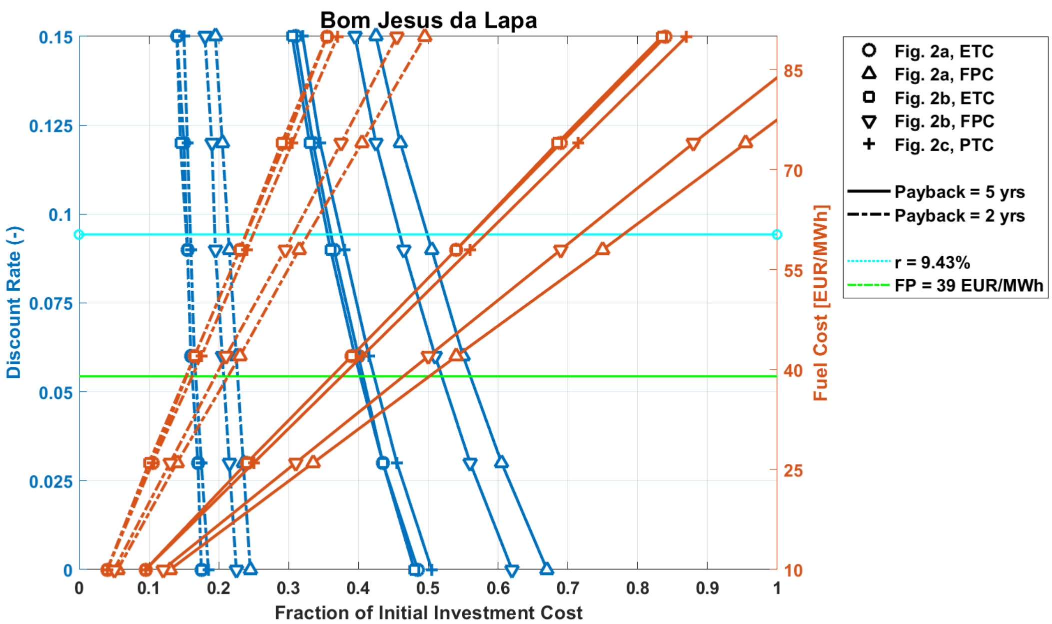

**Fig. 6: Constant payback time curves for each simulated system in Bom Jesus da Lapa, as a function of the reduction in initial investment cost. Curves in blue show the relationship between the discount rate and initial investment for fixed payback times. Orange curves show the relation between conventional fuel cost and initial investment for fixed payback times.**

While the results in these figures can help to compare how different SHIP integration schemes require different capital cost reductions, they offer little information on the actual payback time achieved by these systems. For instance, the results in Fig. 6 show that in Bom Jesus da Lapa fixed collector systems without storage require smaller investment cost reductions than PTC systems. However, actual fuel costs in Bom Jesus da Lapa may differ from the considered average value of 39 €/MWh, and discount rates may differ from the national WACC of 9,43% due to state and federal policies for the region. Furthermore, both fuel costs and discount rates may vary over time because of market changes and government policies. The curves in Fig. 6 are not able to show the required SHIP cost reduction if both the discount rate and the fuel cost are different from the reference values used. It is also worth mentioning that the SHIP system costs considered in this work come mostly from European references, so actual costs in Brazil may be different.

Therefore, the combined influence of fuel costs and discount rate must be considered so that required cost reductions and payback times can be calculated for each simulated SHIP system.

### 3.1. Sensitivity analysis

The final step on the study was to assess how much initial investment costs must be reduced for the SHIP system to reach a given payback time, if both the discount rate and fuel costs vary. The optimal field areas obtained in the Fig. 3 were used to calculate the payback time of the simulated systems, under several discount rate values other than 9,43%, several fuel costs other than 39 €/MWh, and several fractions of the initial investment cost.

So, for instance, the simulation results from the PTC system in Fig. 2c with optimal field area were used to calculate the system payback time under discount rates varying from 0 to 15%, fuel costs varying from 10 to 100 €/MWh, and initial investment costs varying from 1 to 100% of the cost considered in Table 1.

Fig. 7 shows the relation between discount rate (d) and fraction of initial investment cost ($fI_0$) along curves of constant payback times. Each plot in Fig. 7 was generated considering a fixed fuel cost (FC) in €/MWh, for the PTC system of Fig. 2c operating in Bom Jesus da Lapa. Similar results are shown in Figs. 8 and 9, for São Miguel do Oeste and Porto Velho, respectively.

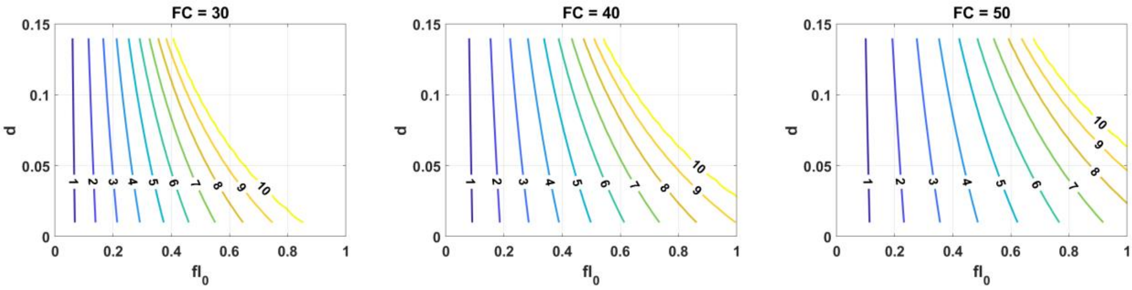


**Fig. 7: Constant payback time curves for fixed fuel costs, for varying discount rate and initial investment cost fraction. Results for the PTC collector system in Fig. 2c, operating in Bom Jesus da Lapa.**

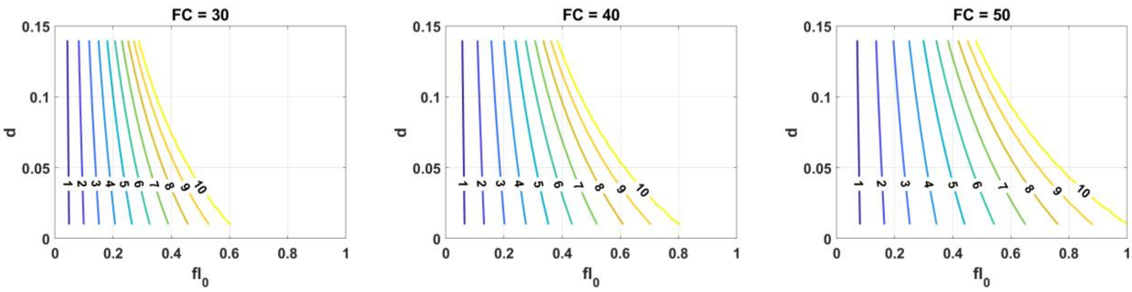


**Fig. 8: Constant payback time curves for fixed fuel costs, for varying discount rate and initial investment cost fraction. Results for the PTC collector system in Fig. 2c, operating in São Miguel do Oeste.**

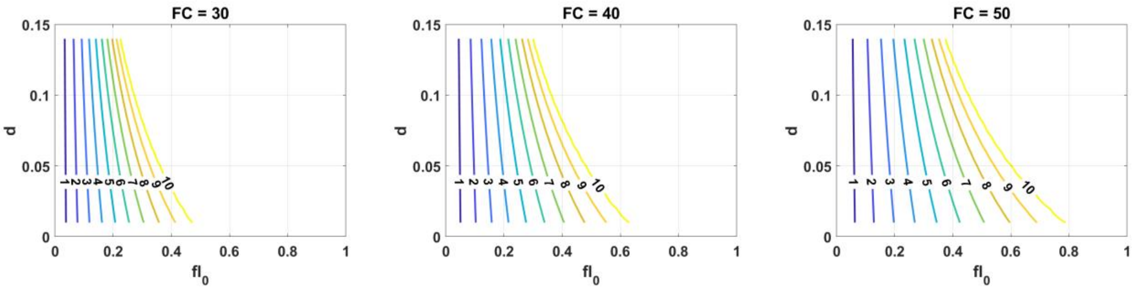


**Fig. 9: Constant payback time curves for fixed fuel costs, for varying discount rate and initial investment cost fraction. Results for the PTC collector system in Fig. 2c, operating in Porto Velho.**

These results show how a decrease in discount rate diminishes the required cost reduction in SHIP and, more importantly, the significant effect of fuel cost on the system profitability. In all three cases, if the fuel cost is slightly lower than the average national cost, 30 €/MWh instead of 39 €/MWh, investment costs must be reduced to 40% or less of its initial value if the PTC system is to reach payback times of up to 5 years, depending on the discount rate. When fuel costs are 50 €/MWh, costs must be reduced to 60% or less in Bom Jesus da Lapa, and 35% or less in Porto Velho.

This highlights another very important barrier for the usage of SHIP in the Brazilian industry: the availability of cheap biomass fuel in the country, especially firewood. Costs for firewood in Brazil vary along the country but can be as low as 10 €/MWh (Solar Payback, 2018), a price against which solar process heat cannot compete. However, even though most of the firewood in Brazil comes from legitimate sources, a significant share (around 25% according to the Solar Payback report) still comes from illegal deforestation. In regions where illegal firewood is still used, solar process heat may prove valuable.

The results for fixed collectors in Figs. 10 to 13 are similar to those obtained for PTC collectors. For a fuel price of 30 €/MWh, costs in Bom Jesus da Lapa must be reduced to as low as 35% in order to achieve payback times of up to 5 years. For São Miguel do Oeste, the costs must be reduced to as low as 20%. This shows that even fixed collector systems, that are cheaper when compared to PTC systems, have difficulty to compete with low fuel prices.

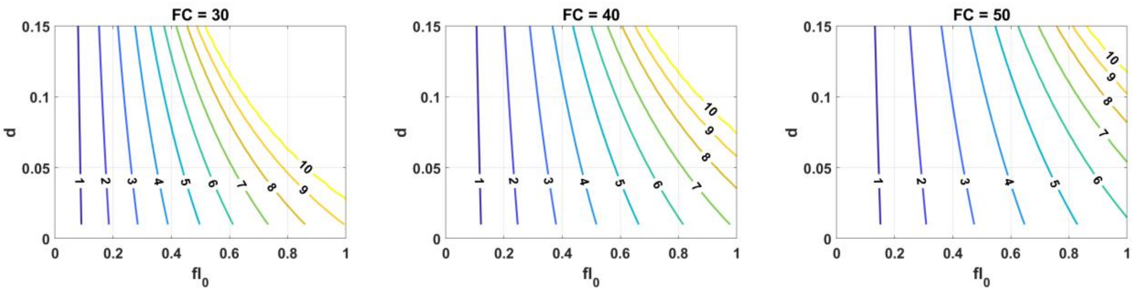


**Fig. 10: Constant payback time curves for fixed fuel costs, for varying discount rate and initial investment cost fraction. Results for the FPC collector system in Fig. 2a, operating in Bom Jesus da Lapa.**

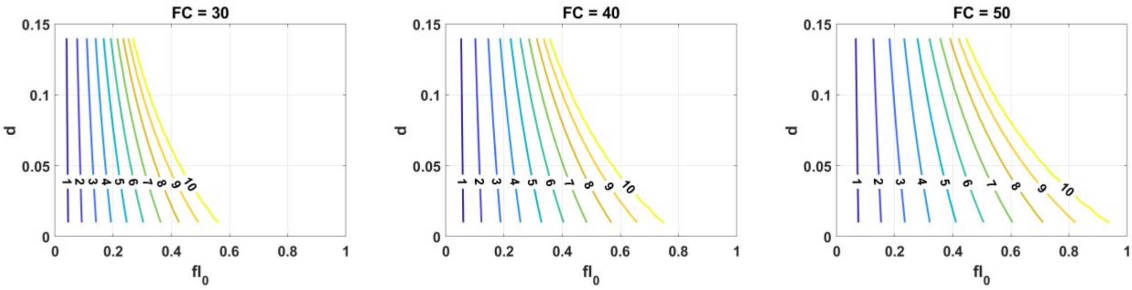


**Fig. 11: Constant payback time curves for fixed fuel costs, for varying discount rate and initial investment cost fraction. Results for the FPC collector system in Fig. 2a, operating in São Miguel do Oeste.**

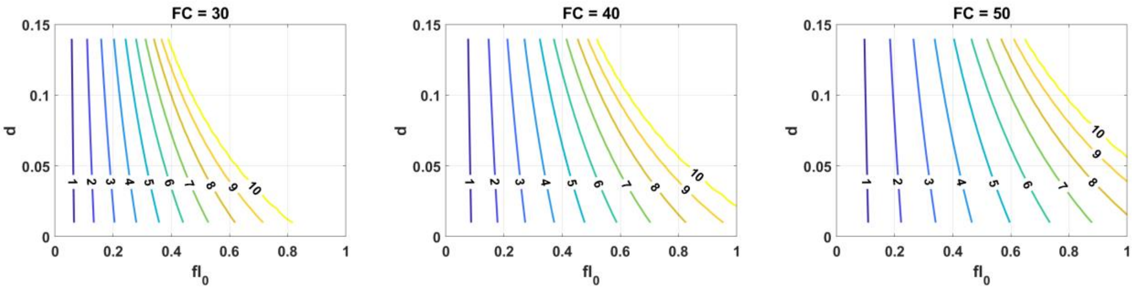


**Fig. 12: Constant payback time curves for fixed fuel costs, for varying discount rate and initial investment cost fraction. Results for the ETC collector system in Fig. 2b, operating in Bom Jesus da Lapa.**

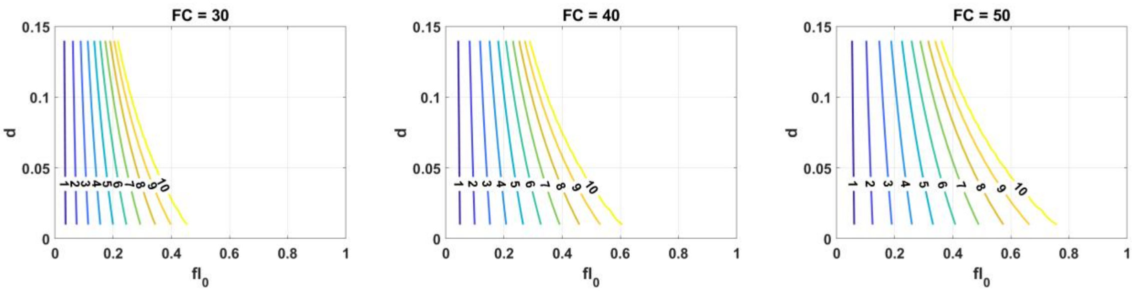


**Fig. 13: Constant payback time curves for fixed fuel costs, for varying discount rate and initial investment cost fraction. Results for the ETC collector system in Fig. 2b, operating in São Miguel do Oeste.**

## 4. Conclusions

The main result from this preliminary study is that the profitability of SHIP systems in Brazil is strongly dependent on the location where solar process heat is to be installed. In locations where cheap biomass fuel is available, the use of SHIP is currently not viable. In other regions of the country where biomass is not easily available, the cost of natural gas or other fuel sources will determine whether SHIP systems can be profitable, depending on future cost reductions of solar system components and on incentives such as subsidization and special financing. A more detailed, nation-wide study is required to better identify the regions of the country where solar process heat can compete with other fuels. Also, a more detailed breakdown of SHIP costs in Brazil can help to identify potential cost reduction strategies. These and other studies will provide further information for policymakers and investors interested in renewable energy in Brazil.

## 5. Acknowledgments

This study was financed in part by the Coordenação de Aperfeiçoamento de Pessoal de Nível Superior – Brasil (CAPES) – Finance Code 001, and by the Conselho Nacional de Desenvolvimento Científico e Tecnológico - CNPq. This work has been developed within the context of all activities related to the R&D project registered with the Agência Nacional de Petróleo, Gás Natural e Biocombustíveis (ANP) under the code 19828-3 and sponsored by Petroleo Brasileiro (PETROBRAS).

## 6. References

ABIA, 2018. Faturamento da Industria de Alimentos 2013 – 2018.
<https://www.abia.org.br/vsn/anexos/faturamento2018.pdf> (accessed on 12 February 2019).

Appsol, 2014. WP3: Caracterización de los Procesos Productivos de las Industrias Manufactureras Chilenas. < http://appsol.cl/wp-content/uploads/2018/04/APPSOL.WP3-Caracterizacio%CC%81n-de-Procesos.pdf > (accessed on 20 February 2019).

Bylund, G., 1995. Dairy Processing Handbook, first ed., Tetra Pak Processing Systems AB, Lund.

Cortés, F., Ibarra, M., Moser, F., Muñoz, I., Crespo, A. and Murray, C., 2017, Techno-economical Evaluation of Parabolic Trough Collector Systems for Steam Processes in the Chilean Industry, Proceedings of the SolarPACES 2017 conference, Santiago, Chile

FAS-USDA, 2018. Dairy production. < https://www.clal.it/en/?section=stat_brasile> (accessed on 15 February 2019).

Goswami, D.Y., Kreith, F. and Kreider, J., 2000. Principles of Solar Energy, second ed., Taylor and Francis Group, New York.

INMET, 2019. BDMEP – Banco de dados metereológicos para ensino e pesquisa. <www.inmet.gov.br/portal/index.php?r=bdmep/bdmep> (accessed on 06 March 2019)

Lemos, L.F.L., Starke, A.R., Boland. J., Cardemil, J.M., Machado, R.D. and Colle, S., 2017. Assessment of solar radiation components in Brazil using the BRL model. Renew. Energy, 108, 569–580.

Louvet, Y., Fischer, S., Furbo, S., Giovanetti, F., Mauthner, F., Mugnier, D., and Philippen, D, 2017. Guideline for levelized cost of heat (LCOH) calculations for solar thermal applications. IEA SHC Task 54: Price Reduction of Solar Thermal Systems. IEA SHC <http://task54.iea-shc.org/Data/Sites/54/media/info-sheets/170306-IEA-SHC_Task%2054-Info_Sheet_LCOH.pdf> (accessed on 06 February 2019).

Machado, R. D, Bravo, G., Starke, A. R., Lemos, L. F. L., Colle, S., 2017. Generation of 441 typical meteorological year from INMET stations in Brazil. Proceedings of the SWC 2019/SHC 2019. Santiago, Chile

Mane, S. R., 2013. Energy management in a dairy industry. Int. J. Mech. Prod. Eng., 1, 27–32.

Mauthner, F. and Herkel, S., 2016. Technical Report Subtask C – Part C1: Classification and Benchmarking of Solar Thermal Systems in Urban Environments. IEA SHC Task 52: Solar Thermal Applications in Urban Environments. IEA SHC <task52.iea-shc.org/Data/Sites/1/publications/IEA-SHC-Task52-STC1-Classification-and-Benchmarking_v02.pdf > (accessed on 17 March 2019).

Quijera, J. A., Alriols, M. G and Labidi, J., 2011. Integration of a solar thermal system in a dairy process. Renew. Energy, 36, 6, 1843–1853.

Rahimi, B. and Chua, H. T., 2017. Low grade heat driven multi-effect distillation and desalination, first ed. Elsevier, Amsterdam.

Rocha, K., Gutierrez, M. B. G. P. S., Hauser, P. A remuneração dos investimentos em energia renovável no brasil – Uma proposta metodológica ao *Benchmark* da UNFCCC para o Brasil. < http://www.ipea.gov.br/portal/images/stories/PDFs/TDs/td_1701.pdf> (accessed on 13 March 2019).

Silva, P. C., 2014. Gestão da energia na indústria de laticínios. <http://repositorio.unicamp.br/jspui/bitstream/REPOSIP/265894/1/Silva_PauloCesar_M.pdf> (accessed on 10 February 2019).

Solar Keymark, 2019. Collector Certificates.<http://www.solarkeymark.dk/CollectorCertificates> (accessed on 04 March 2019)

Solar Payback, 2018. Energia Termossolar para a Indústria: Brasil. <https://www.solar-payback.com/wp-content/uploads/2018/08/SHIPBrasil-PT2018_FINAL.pdf> (accessed on 06 February 2019).

Sokhansefat, T., Kasaeian, A., Rahmani, K., Heidari, A.H., Aghakhani, F. and Mahian, O., 2018. Thermoeconomic and environmental analysis of solar flat plate and evacuated tube collectors in cold climatic conditions. Renew. Energy, 115, 501–508.

SPF, 2019. Solar Collector Factsheet NEP PolyTrough 1800. <http://www.spf.ch/fileadmin/daten/reportInterface/kollektoren/factsheets/scf1549de.pdf> (accessed on 04 March 2019).

TESS, 2014. TESS Libs 17 - Component Libraries for the TRNSYS Simulation Environment. High Temperature Solar Library and Solar Library.

Tian, Z., 2017. Performance and Optimization of a Novel Combined Solar Heating Plant with Flat Plate Collectors and Parabolic Trough Collectors in Series for District Heating. In: Proceedings of SWC2017/SHC2017, 1–3.

Ulrich, G.D. and Vasudevan, P.T., 2004. Chemical engineering process design and economics: a practical guide, second ed., Process Publishing, Durham.

VDI-Gesellschaft. VDI Heat Atlas. Second Edition. Springer, 2010.

World Bank Group, 2019. Global Solar Atlas. <https://globalsolaratlas.info/> (accessed on 28 June 2019).